Dual band antireflection coatings for the infrared

Thomas D. Rahmlow, Jr.*[a], Jeanne E. Lazo-Wasem[a], Scott Wilkinson[b], and Flemming Tinker[c]
[a]Rugate Technologies, Inc., 353 Christian Street, Oxford, CT 06478;
[b]Corning Specialty Materials, 69 Island Street, Keene, NH 03431;
[c]Flemming Tinker, LLC, 23 Soobitsky Road, Higganum, CT 06441

Proc. SPIE 10524, Free-Space Laser Communication and Atmospheric Propagation XXX, 1052416 (2018);
doi:10.1117/12.2290753

Dual band antireflection coatings for the infrared

Thomas D. Rahmlow, Jr.*[a], Jeanne E. Lazo-Wasem[a], Scott Wilkinson[b], and Flemming Tinker[c]
[a]Rugate Technologies, Inc., 353 Christian Street, Oxford, CT 06478;
[b]Corning Specialty Materials, 69 Island Street, Keene, NH 03431;
[c] Flemming Tinker, LLC, 23 Soobitsky Road, Higganum, CT 06441

ABSTRACT

Sensor performance for dual band forward looking infrared (FLIR) imagers can be substantially improved by increased simultaneous throughput of both sensor bands in the optical systems. Currently available antireflection coatings (ARs) have optimized performance for either spectral band, but not both on the same optic. Where AR coatings cover the mid and long wave infrared (LWIR) bands, or the entire broad band spectrum from visible to LWIR, performance is not sufficient for future systems. A method of designing and fabricating high performance ARs has been developed. This paper presents a discussion of the trade-off of film thickness and complexity versus transmission performance. Fabrication results for high, medium and low index lens materials are also presented.

Keywords: antireflection, dual band, infrared, interference coating, rugate, broad band

1. INTRODUCTION

The development of dual band infrared sensors with optics that share a common aperture creates the need for high performance optical coatings in multiple spectral bands[1]. This new generation of IR imagers can have 10 or more surfaces and use a selection of high to low refractive index lens materials. High performance, dual band anti-reflection coatings that reduce surface reflection to less than 1% per surface in each spectral band for these materials are required to maximize system sensitivity. Dual band IR coatings are typically thicker and more complicated than anti-reflection coatings which have been optimized for either the mid-IR (3.5 to 5μm) or far-IR (7.8 to 10.5μm) spectral bands.

Figure 1 presents the real part of the refractive index for a number of materials used in the design of an infrared refractive optics system [2,3,4]. Optics fabricated from high index materials such as germanium (Ge) exhibit reflection losses of 53% prior to AR coating both surfaces. The reflection losses of low index fluoride optics are considerably less, typically 6 to 8%, but can still contribute to significant degradation in a system comprised of many refractive components. Figure 2 presents the modeled transmission for a germanium window coated with a dual band IR antireflection film on both surfaces.

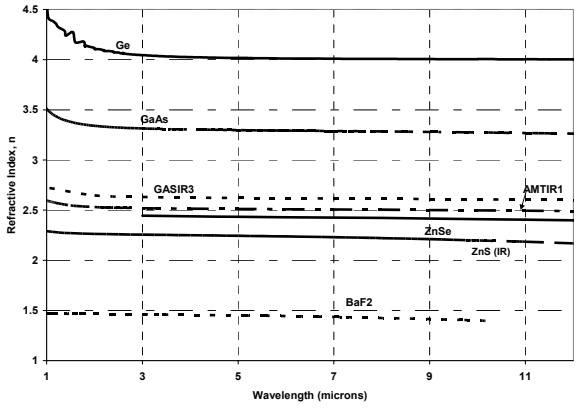

Figure 1: The refractive index for a Ge, Si, AMTIR, ZnSe, ZnS, CaF_2 and BaF_2 are presented as a function of wavelength.

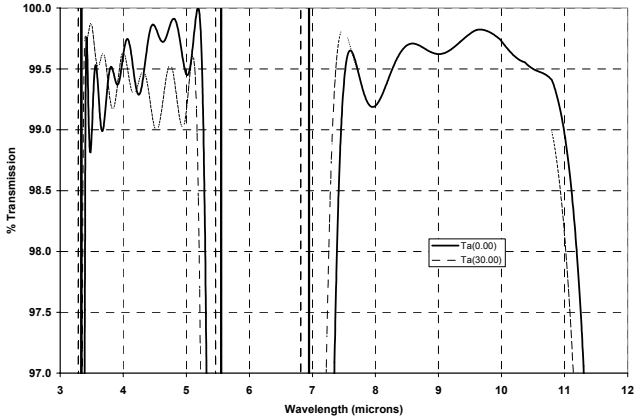

Figure 2: Modeled transmission and reflection for a dual band AR on germanium. Both surfaces are coated.

Infrared Technology and Applications XXXIV, edited by Bjørn F. Andresen, Gabor F. Fulop, Paul R. Norton,
Proc. of SPIE Vol. 6940, 69400T, (2008) · 0277-786X/08/$18 · doi: 10.1117/12.780288

2. DESIGN APPROACH FOR DUAL BAND AR FILMS

Many of the materials that are appropriate as refractive optical components for infrared applications have moderate to high refractive index values which give rise to high Fresnel reflection losses. A single germanium surface has a reflection loss of 36%. An anti-reflection coating can reduce the optical reflection significantly over a limited spectral region. Single band anti-reflection interference coatings of 4 to 7 layers can reduce the single surface reflection of germanium to less than 0.5% over a spectral range of 7.5 to 12μm. However, when transmission over multiple ranges or a broad range is required, the high performance coating design becomes more complex, and more challenging to fabricate.

A contemporary approach to computer aided coating design is needle synthesis. The needle synthesis method begins with a starting design which could be a legacy design or simply a single layer of one of the available thin film material set. A performance target is described and a thin needle of material is systematically inserted along the thickness of the starting design. A performance merit is calculated at each insertion point, and the thin layer is inserted at the point where the needle most reduces the performance merit function[5]. The performance merit is the root-mean-square of the deviations between predicted performance and the performance target. The new design, now two or three layers if a single layer starting design was used, is refined, allowing the layers to change in optical thickness so as to further reduce the merit function. The process is repeated inserting a new layer and refining the design until the insertion of any thin layer does not reduce the merit function.

Needle synthesis is a powerful method for producing designs with complex performance. However, while the method can produce acceptable solutions, it can just as easily produce solutions which are not easy to manufacture, or which contain a large number of layers and fabrication time would prohibitively drive coating cost. Understanding the design trade-offs of film thickness, number of layers and the choice of coating materials can significantly impact coating complexity and cost.

2.1 Discrete Antireflection Films for ZnSe

Figures 3 through 12 support the following discussion of antireflection films for zinc selenide (ZnSe) substrates. ZnSe has a medium refractive index of 2.43 in the infrared. Figure 3 presents a 5 layer discrete AR film for the far-IR region. This design reduces the reflection from 7.5 to 11μm to less than half a percent at normal and 30^{o} angle of incidence (AOI). The impact of using this AR on ten surfaces in the system is presented in figure 4. A dual band design of comparable thickness and complexity is presented in figure 5. This is a 6 layer design using the same coating materials as the single band AR presented in figure 6. The significant impact of this design on total system performance is presented in figure 6.

The film thickness, the index contrast of the selected materials and the number of layers in the design constitute the design space for the AR films. In order to improve the performance of the dual band AR presented in figure 5, the design space must be extended. The challenge is to find an optimal solution which meets the performance specifications, but does not over tax the fabrication process. The issue is to find a practical range of film thicknesses and number of layers which meet the goal of less than 1% reflection in both spectral bands. A secondary issue is to seek out a set of coating materials that can be used for the full range of substrate types. This allows for standardization of the fabrication process and reduced production costs. The materials used for these designs are zinc sulfide (ZnS) and yttrium fluoride (YF3) for the medium and low index materials and germanium (Ge) for the high index material.

The use of a third material in a design has the potential of expanding the design space and improving the performance of the film with out adding significantly to design complexity. Figures 7 and 9 present modeled performance of 2 and 3 material designs. Both designs are more complex then the previous dual band design. The designs are 15 layers and are twice as thick as the previous design. The need for improved performance drives the complexity of the design, and this trade-off in performance versus design space is presented in figures 11 and 12 for the 2 material design set and in figures 13 and 14 for the three material design set. Figure 11 plots the number of layers and the total film thickness as a function of the optimization value of merit. The designs chosen for closer examination are those near the knee of the curve as they are typically the best performance for the least complexity (fewest number of layers and least film thickness).

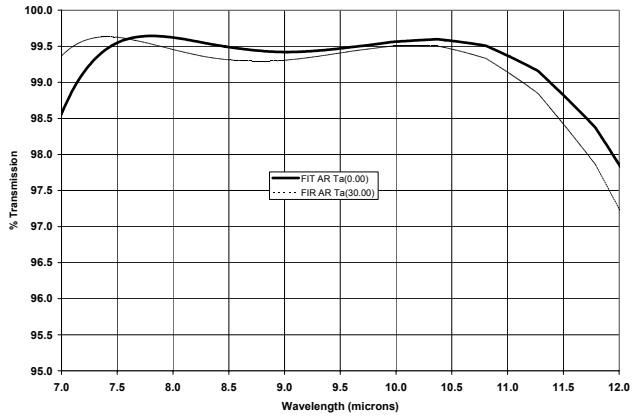

Figure 3: Single Band (FIR) 5 layer discrete on ZnSe. The film is 2.6 microns thick. Modeled performance at 0 and 30^{o} AOI is presented.

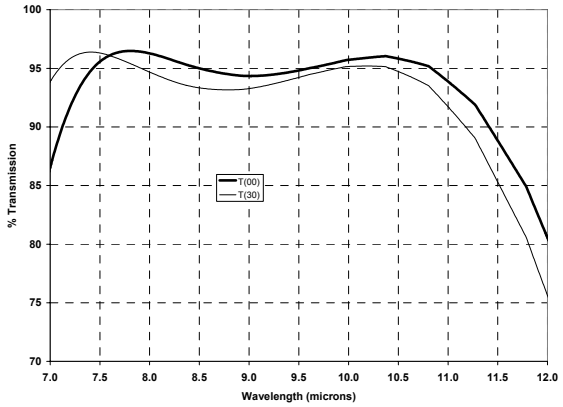

Figure 4: System Impact (10 surfaces) of the single band FIR AR is plotted at normal and 30^{o} AOI.

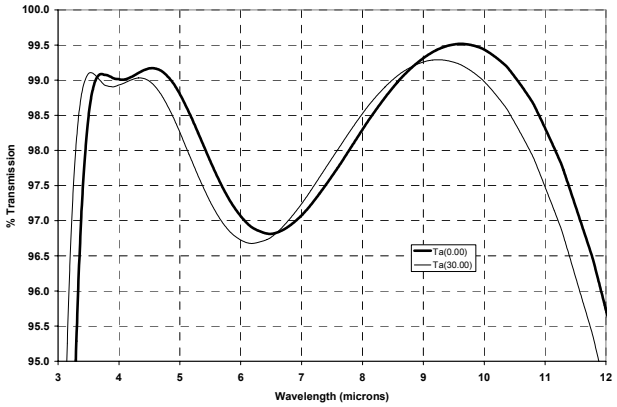

Figure 5: Dual Band 6 layers discrete modeled for 0 and 30^{o} AOI.

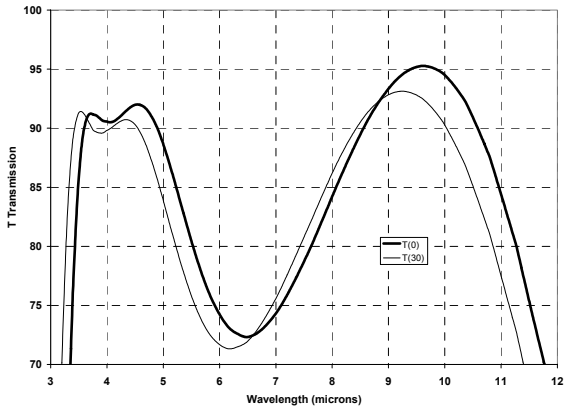

Figure 6: System Impact (10 surfaces) for a 6 layer dual band AR of comparable thickness as the single band FIR AR.

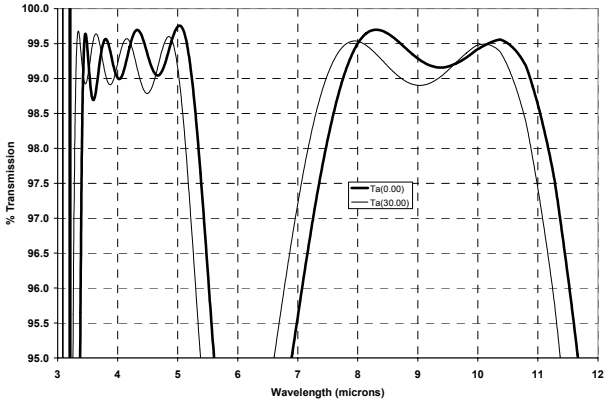

Figure 7: Dual Band 15 layers, 2 material discrete: 0, 30^{o} AOI, medium/low index materials

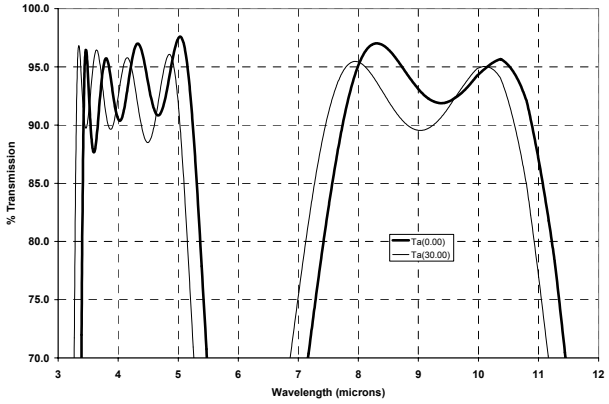

Figure 8: System Impact (10 surfaces) for a 15 layer dual band AR.

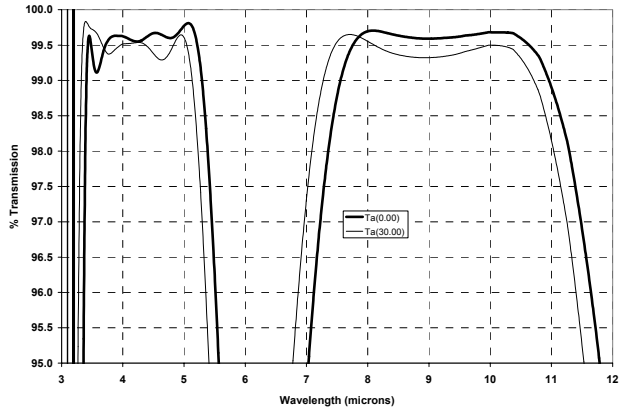

Figure 9: Dual Band 15 layers, 3 material discrete: 0, 30° AOI

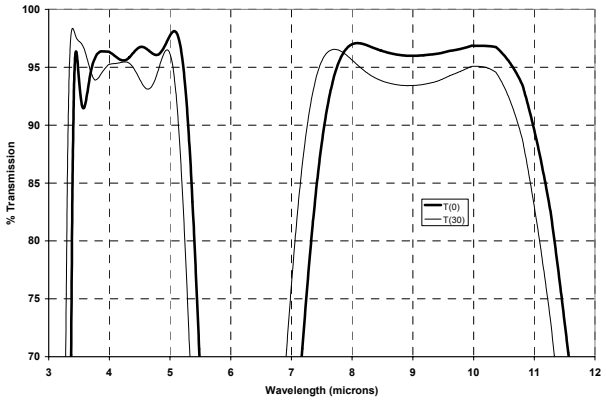

Figure 10: System Impact (10 surfaces) for a 15 layer 3 material AR modeled for 0 and 30° AOI.

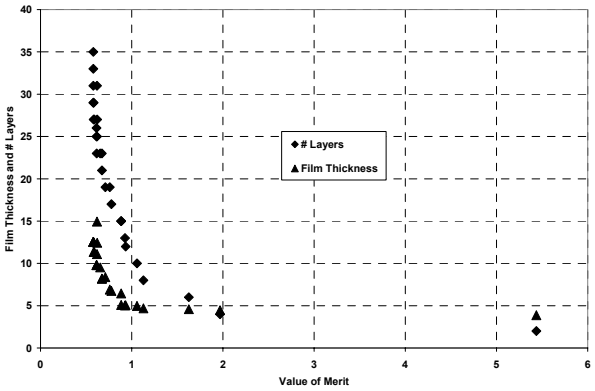

Figure 11: Film thickness and the number of layers in the design are plotted against the optimization value of merit for a series of two material (ZnS/YF_3) AR designs for ZnSe.

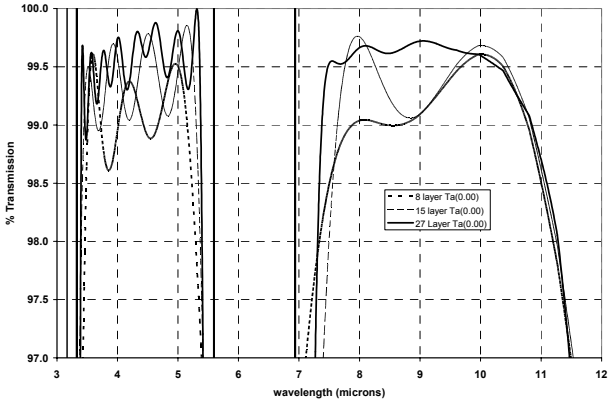

Figure 12: Modeled transmission for dual band AR designs of different number of layers and thickness are compared for two material AR designs for ZnSe.

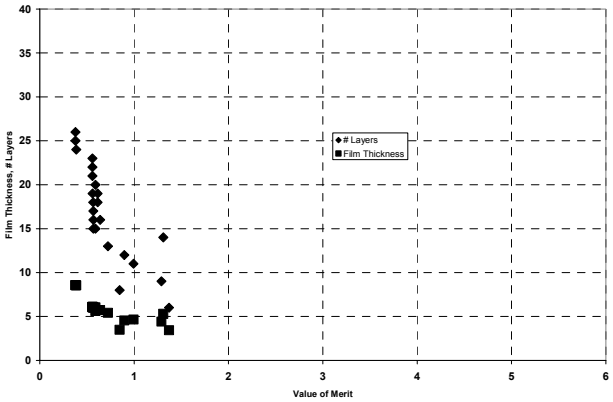

Figure 13: Film thickness and the number of layers in the design are plotted against the optimization value of merit for a series of three material (ZnS/YF_3) AR designs for ZnSe.

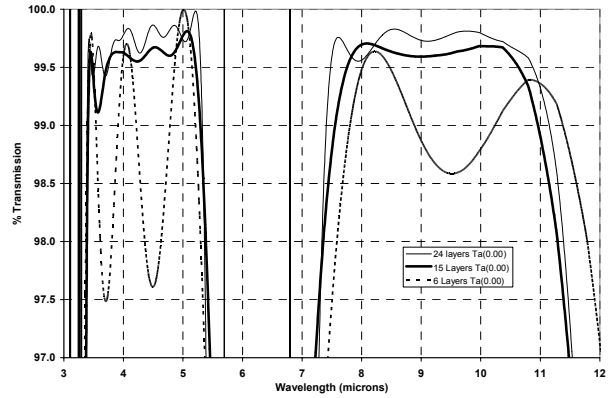

Figure 14: Modeled transmission for dual band AR designs of different number of layers and thickness are compared for three material AR designs for ZnSe.

Figures 11 and 13 present a visualization of the trade-off between performance and design complexity. The design performance improves with an initial increase in film thickness and the number of layers. However, the improvement in film performance becomes increasingly small and the slope of the trend changes from nearly horizontal to nearly vertical. The diminishing return for increased complexity is illustrates in the transmission plots of figures 12 and 14.

Table 1 presents a summary of the designs presented in figures 12 and 14. For the 2-material design, improving the performance from 99.3% to 99.5% requires doubling the thickness of the design and nearly doubling the number of film layers.

Table 1: Summary of Design Performance for 2 and 3 Material ZnSe Dual AR Designs;

Material	Layers	Thickness (µm)	Merit	Film Only Ave MIR %T	Film Only MIR Transmission loss (1-T)	Film Only Ave FIR %T	Film Only FIR Transmission loss (1-T)
ZnS/YF3	8	4.69	1.1296	99.02	0.98	99.17	0.83
	15	6.46	0.8670	99.32	0.68	99.34	0.66
	27	12.50	0.5817	99.54	0.46	99.54	0.46
Ge/ZnS/YF3	6	3.45	1.3702	98.60	1.40	99.08	0.92
	15	6.03	0.5906	99.53	0.47	99.59	0.41
	24	8.55	0.3861	99.72	0.28	99.71	0.29

2.2 Dual Band AR performance by Substrate Type

Using the design approach previously described, dual band AR film designs for Ge, AMTIR, ZnSe, ZnS, CaF_2 and BaF_2 were developed and are presented in figures 15 through 20. Film characteristics are summarized in Table 2. All designs are in the range of 5 to 7 microns thick and 14 to 20 layers.

Table 2: Summary of Predicted AR Transmission for a 1 mm Substrate Coated on Both Surfaces

Substrate	Total Thickness	# Layers	Ave 3.5-5 µm	Ave Transmission loss (1-T), 3.5-5µm	Ave 7.8-10.5 µm	Ave Transmission loss (1-T) 7.8-10.5µm
Ge	6.72	18	99.27	0.73	98.90	1.10
AMTIR	6.08	15	98.13	1.87	97.88	2.12
ZnSe	6.03	15	99.03	0.97	99.18	0.82
ZnS	6.37	15	99.33	0.67	98.93	1.07
BaF_2	4.57	13	98.57	1.43	98.33	1.67
CaF_2	4.61	13	96.46	3.54	71.90	28.10

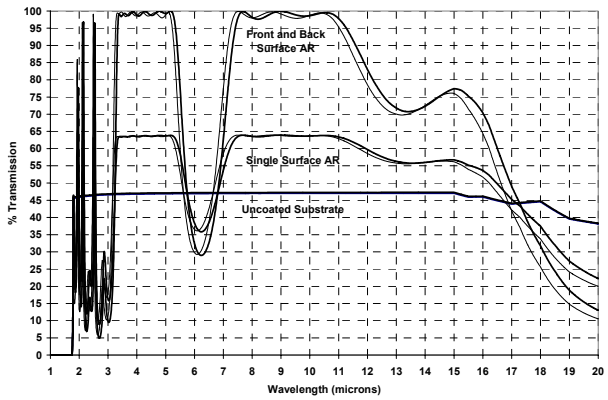

Figure 15: Ge AR transmission is modeled on a 1 mm thick germanium substrate. Uncoated, single surface and dual surface coated germanium is presented at normal and 30° AOI.

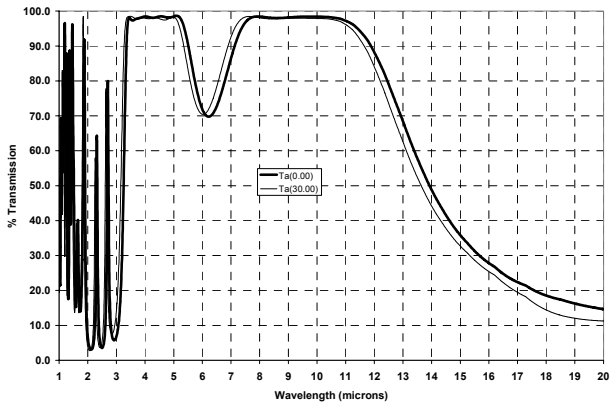

Figure 16: AMTIR AR transmission is modeled for a 1 mm thick AMTIR substrate

Figure 17 and 18 present the ZnSe design again, but examine the angle response of the film. Figure 17 is modeled at 0, 10, 20, 30, 40, 50 and 60 ^{o} AOI. Average transmission for each spectral band is presented as a function of angle in figure 18. The transmission for both bands remains flat out to the design angle of 30^{o} and then rolls off at higher angle.

Figure 20 presents an overlay of modeled performance for a dual band AR for CaF2 and BaF2. This is a plot of transmission for only the film. CaF2 absorbs significantly above 9.5 microns and is not typically used for FIR applications. It is included here only as a low index test substrate.

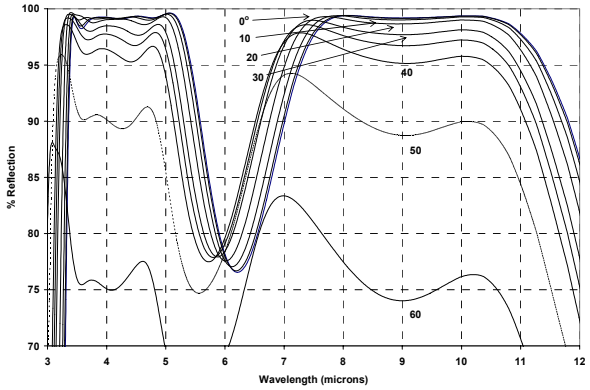

Figure 17: ZnSe AR performance for a range of angles of incidence from normal to 60^{o}.

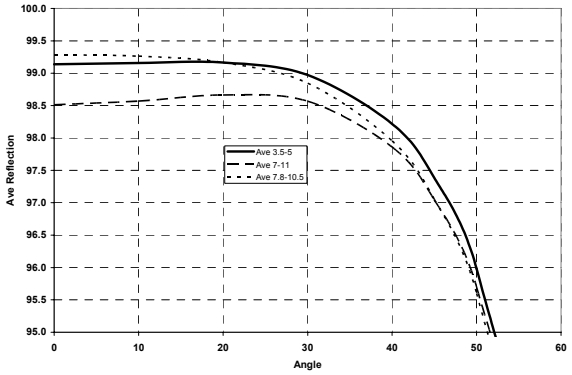

Figure 18: ZnSe AR average transmission in the mid and far IR bands is plotted as a function of angle.

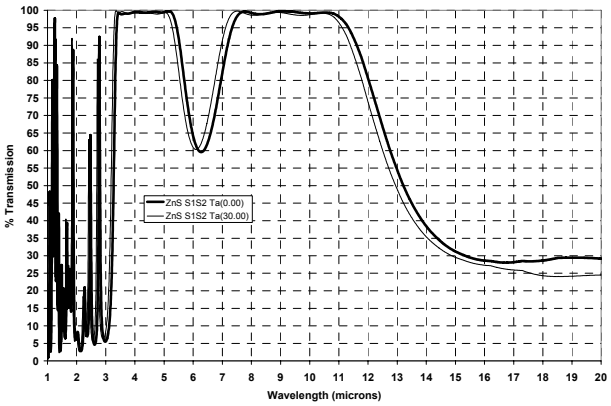

Figure 19: Figure 20: ZnS modeled transmission at 0 and 30^{o} AOI. The 1mm substrate is modeled with the AR on both surfaces.

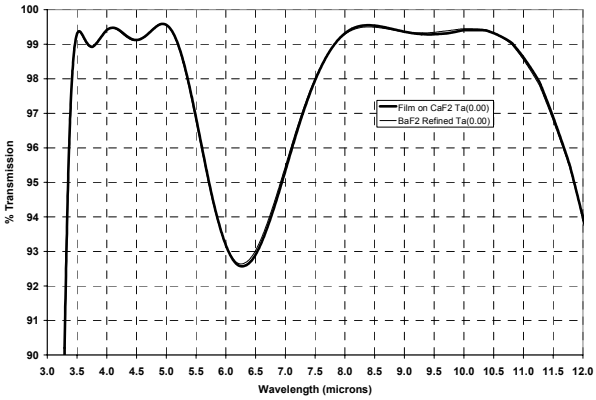

Figure 21: CaF2 and BaF2 - comparison of the CaF2 Dual Band AR on CaF2 and the BaF2 AR refined for BaF2 on BaF2. Both films are 13 layers. The modeled transmission is the film only. Substrate absorption is not included.

3. FABRICATION RESULTS

Germanium, AMTIR, ZnSe and CaF_2 were selected for test fabrication runs. Witness parts are 1" diameter and 1 mm thick, with the exception of AMTIR, which is 2mm thick. Figures 21 through 26 present measured spectral results for each of the substrates. The selected coatings were deposited on both surfaces. Transmission and reflection measurements include substrate and film absorption when present. Table 3 summarizes film performance.

Table 3: Summary of Measured AR Performance

Lens Material	Measurement	Average % Transmission (loss)	
		3.5 to 5µm	7.8 to 10.5µm
Ge	% T (0°), % R(10°)	97.3 (2.7)	96.8 (3.2)
	% T at 30°	95.9 (4.1)	96.3 (3.7)
AMTIR	% T (0°), % R(10°)	98.4 (1.6)	97.9 (2.1)
	% T at 30°	95.3 (4.7)	95.8 (4.2)
ZnSe	% T (0°), % R(10°)	98.0 (2.0)	97.6 (2.4)
	% T at 30°	97.9 (2.1)	99.0 (1.0)
CaF2	% T (0°), % R(10°)	96.3 (3.7)	89.7 (10.3)
	% T at 30°	97.6 (2.4)	88.6 (11.4)

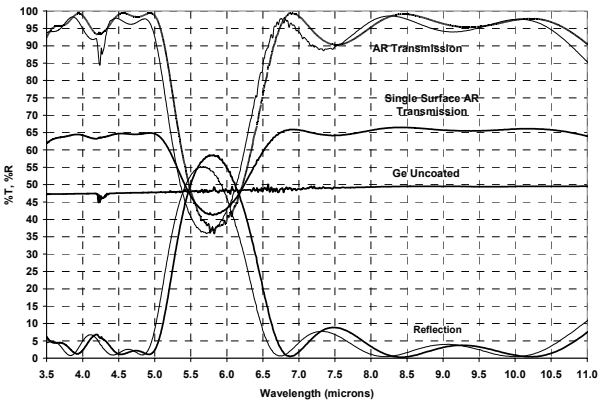

Figure 22: Measured transmission and reflection for the Ge 3-material design on both surfaces of a 1 mm thick witness part.

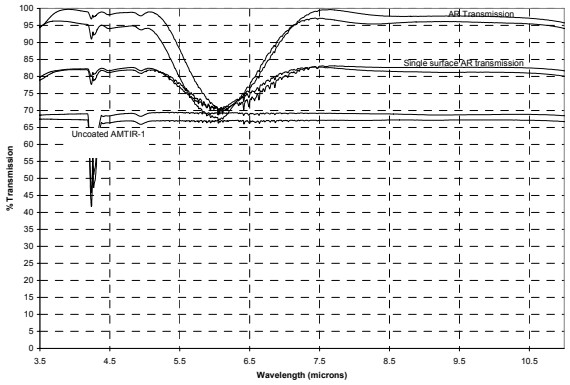

Figure 23: Measured transmission for the AMTIR 3-material design on both surfaces of a 2 mm thick witness part.

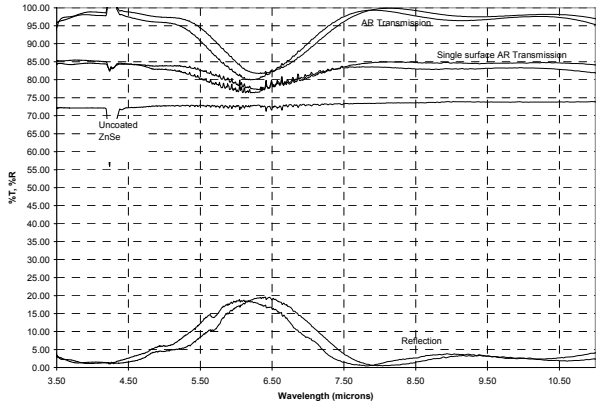

Figure 24: Measured transmission and reflection for the ZnSe 2-material design on both surfaces of a 1 mm thick ZnSe witness part.

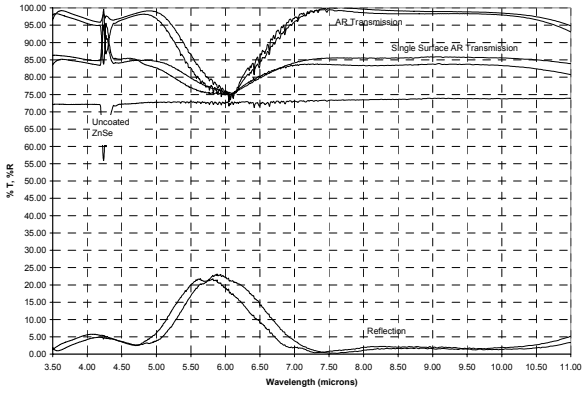

Figure 25: Measured transmission and reflection for the ZnSe 3-material design on both surfaces of a 1 mm thick ZnSe witness part.

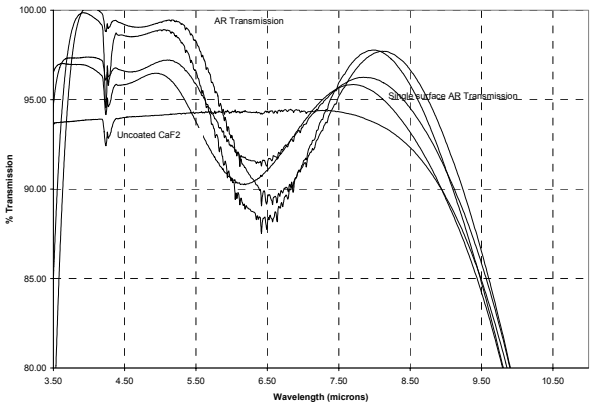

Figure 26 : Measured transmission for the CaF2 2-material design on both surfaces of a 1 mm thick CaF2 witness part.

4. CONCLUSIONS

High performance dual band AR coatings are more complex and thicker than single band AR coatings, but performance in both bands can be designed and fabricated to performance levels comparable to single band AR coatings. A common set of coating materials can be used to cover lens materials with very different refractive index values. The fabricated films exhibit good spectral performance and cosmetic quality. The goal of less than 1% reflection in the both bands is a practical specification.

REFERENCES

[1] Hall, J., "Army Applications for Multi-Spectral Windows", Proc. SPIE 3060, 330-334 (1997).
[2] Palik, E. D., [Handbook of Optical Constants in Solids], Academic Press (1985).
[3] Hilton, Sr., A.R., "Precise refractive index measurements of infrared materials", Proc. SPIE 1307, 516-521 (1990).
[4] "GASIR®3 – Infrared transmitting glass", Umicore Electro-Optical Materials' Product Literature, www.optics.umicore.com
[5] "Advanced Thin-Film Optical Coatings; Evaluation and Design", OptiLayer Ltd., Product literature (1998).
[6] Rahmlow, T. D., Lazo-Wasem, J. E., Gratrix, E. J., "Narrow band infrared filters with broad field of view", Proc. SPIE 6206, 62062S-1 – 62062S-8 (2006).
[7] Vizgaitis, J., "Dual f/number optics for 3rd generation FLIR systems", Proc. SPIE 5783, 875-886 (2005).
[8] Norton, P., Campbell, J., Horn, S., Reago, D., "Third-generation imagers", Proc. SPIE 4130, 226-236 (2000).
[9] Harris, D, [Materials for Infrared Windows and Domes], SPIE Optical Engineering Press (1999).
[10] Hawkins, G., Hunneman, R., "The temperature dependent spectral properties of filter substrate materials in the far-infrared (6-40 μ)", Infrared Physics and Technology 45,69-79, Elsevier (2004).